Published in final edited form as:
Transl Stroke Res. 2020 October ; 11(5): 1064–1076. doi:10.1007/s12975-020-00786-0.

Modeling Mixed Vascular and Alzheimer's Dementia Using Focal Subcortical Ischemic Stroke in Human ApoE4-TR:5XFAD Transgenic Mice

Eric Y. Hayden[1], **Julia M. Huang**[1], **Malena Charreton**[1], **Stefanie M. Nunez**[1], **Jennifer N. Putman**[1], **Bruce Teter**[1], **Jason T. Lee**[2], **Andrew Welch**[3], **Sally Frautschy**[1], **Gregory Cole**[1], **Edmond Teng**[1], **Jason D. Hinman**[1]

[1]Department of Neurology, David Geffen School of Medicine, University of California Los Angeles, 635 Charles E. Young Dr. South, Neuroscience Research Building, Rm 415, Los Angeles, CA 90095, USA

[2]Crump Institute for Molecular Imaging, University of California Los Angeles, Los Angeles, CA 90095, USA

[3]The Institute of Medical Sciences, University of Aberdeen, Aberdeen, UK

Abstract

Subcortical white matter ischemic lesions are increasingly recognized to have pathologic overlap in individuals with Alzheimer's disease (AD). The interaction of white matter ischemic lesions with amyloid pathology seen in AD is poorly characterized. We designed a novel mouse model of subcortical white matter ischemic stroke and AD that can inform our understanding of the cellular and molecular mechanisms of mixed vascular and AD dementia. Subcortical white matter ischemic stroke underlying forelimb motor cortex was induced by local stereotactic injection of an irreversible eNOS inhibitor. Subcortical white matter ischemic stroke or sham procedures were performed on human ApoE4-targeted-replacement (TR):5XFAD mice at 8 weeks of age. Behavioral tests were done at 7, 10, 15, and 20 weeks. A subset of animals underwent ^{18}FDG-PET/CT. At 20 weeks of age, brain tissue was examined for amyloid plaque accumulation and cellular changes. Compared with sham E4-TR:5XFAD mice, those with an early subcortical ischemic stroke showed a significant reduction in amyloid plaque burden in the region of cortex overlying the subcortical stroke. Cognitive performance was improved in E4-TR:5XFAD mice with stroke compared with sham E4-TR:5XFAD animals. Iba-1+ microglial cells in the region of cortex overlying the subcortical stroke were increased in number and morphologic complexity compared with sham E4-TR:5XFAD mice, suggesting that amyloid clearance may be promoted by an interaction between activated microglia and cortical neurons in response to subcortical stroke.

Jason D. Hinman jhinman@mednet.ucla.edu.

Compliance with Ethical Standards

Conflict of Interest The authors declare that they have no conflict of interest.

Ethical Approval All applicable international, national, and institutional guidelines for the care and use of animals were followed.

Electronic supplementary material The online version of this article (https://doi.org/10.1007/s12975-020-00786-0) contains supplementary material, which is available to authorized users.

This novel approach to modeling mixed vascular and AD dementia provides a valuable tool for dissecting the molecular interactions between these two common pathologies.

Keywords

Alzheimer's disease; Amyloid; Lacunar stroke; White matter disease; Modeling; animal models of human disease; inflammation; ischemia; cognitive impairment; cerebrovascular disease/stroke

Introduction

Alzheimer's disease (AD) and vascular dementia account for over 80% of dementia diagnoses. At autopsy, approximately 50% of dementia patients have mixed pathologies, demonstrating hallmarks of chronic cerebrovascular disease along with AD pathology [1]. The most common neuropathologic finding in vascular dementia is focal microvascular ischemic stroke lesions in subcortical white matter that accumulate over time [2]. Similar to AD, white matter ischemic injury is progressive [3] and currently accepted stroke prevention strategies have failed in clinical trials [4]. Despite the common nature of these age-related impairments, surprisingly little effort has focused on understanding how these two pathologies interact at the basic neurobiologic level.

The available neuropathologic and neuroimaging evidence suggests that these pathologies do interact with each other, though the directionality of that interaction is unclear. White matter hyperintensities present on magnetic resonance imaging correlate with the degree of AD pathology in patients [2], while imaging studies of dominantly inherited AD subjects, prior to the expected onset of AD, suggests that subcortical white matter injury predates the clinical development of dementia symptomatology by as much as 22 years [5]. However, cerebrovascular pathology was significantly higher in a cohort of sporadic AD subjects compared with those with autosomal-dominant AD [6]. More recent studies find that subjects with pathologic features of AD and cerebrovascular pathology had less impairment and slower decline [7], complicating the simple interpretation that these lesions synergize to worsen cognitive impairment. This high degree of co-morbidity implies a neurobiologic link, yet no clear molecular relationship has been established between the two disorders.

Several hypotheses have been suggested to establish a link between cerebrovascular pathology and AD including low-level chronic inflammation provoked by white matter injury [8], impaired clearance of the amyloid β-protein(Aβ) through chronically diseased cerebral blood vessels [9, 10], and an axonal molecular death pathway triggered by amyloid precursor protein (APP) [11]. None of the proposed mechanisms have been adequately modeled in vivo with methodologies that accurately reflect the most commonly observed pathologies. Further, past models designed to address the overlap between brain ischemia and AD neurodegenerative phenomena [12–14] failed to consider a time course that reflects the chronic nature of either subcortical white matter ischemic lesions or dementia.

To help identify synergistic biologic pathways between subcortical white matter ischemic stroke and Alzheimer's disease pathology, we developed a novel mouse model of both pathologies by combining a human ApoE4-targeted replacement:5XFAD transgenic mouse

strain (hApoE4-TR:5XFAD) with an established focal white matter ischemic stroke model that mimics human lacunar infarction [15, 16]. This model of subcortical white matter ischemia produces a focal stroke lesion precisely in brain white matter, provokes a focal inflammatory response, and results in a loss of axons and oligodendrocytes [17]. Importantly, this stroke model damages only subcortical white matter axons while allowing investigations of the effect of this lesion on connected and surviving cortical neurons [15, 18].

In this initial attempt at modeling subcortical white matter ischemic injury and AD-related neuropathology, we chose to use a human ApoE4-targeted replacement:5XFAD transgenic mouse model because a similar strain has a robust but temporally delayed amyloid accumulation rate compared with the 5XFAD strain [19]. This temporal delay of amyloid accumulation mediated by the human ApoE4 allele allowed us to determine the combined effect of subcortical white matter stroke and AD pathologies along a chronic time scale. Using this paradigm, we determined how the introduction of a subcortical white matter ischemic stroke prior to the development of significant amyloid pathology in hApoE4-TR:5XFAD mice modifies amyloid generation, cortical inflammation, motor recovery, and cognitive impairment. In this novel model of mixed vascular and AD dementia, we find that subcortical white matter stroke reduces amyloid plaque accumulation in the cortex overlying the white matter lesion. This local reduction in amyloid is associated with an altered inflammatory state of the overlying cortex triggered by subcortical stroke. These cellular and molecular events are associated with modest improvements in motor recovery after stroke in the mixed model as well as a partial rescue of deficits in cognitive impairment associated with the 5XFAD transgene. These seemingly paradoxical results indicate that prevailing hypotheses that mixed pathologies necessarily result in accelerated dementia and amyloidogenesis may not be true and deserve additional study in animal models that aim to more precisely model mixed vascular and Alzheimer’s dementia.

Methods

Transgenic Animals

All animal studies presented here were approved by the UCLA Animal Research Committee, accredited by the AAALAC. ApoE-TR mice which express the human ApoE4 allele under the control of the endogenous mouse ApoE promoter [20] were bred to 5XFAD mice which co-express five FAD mutations (*APP* K670N/M671L+I716V+V717I and *PS1* M146L+L286V) under the control of the neuron-specific mouse Thy-1 promoter [21], and backcrossed to ApoE-TR mice, resulting in mice homozygous for *APOE4*, and hemizygous for the 5XFAD transgenes. Mice were then inbred between 5xFAD+ and 5xFAD− resulting in littermates E4+/+:FAD+ (E4-TR:FAD+) and E4+/+:FAD− (E4-TR:FAD−).Animals were genotyped using established PCR and qPCR assays (Transnetyx) [21, 22]. One cohort of ER-TR:FAD+ mice were used to assess pathologic changes after stroke or sham procedure. A second cohort of offspring including E4-TR:FAD+ and E4-TR:FAD−were utilized for tissue and behavioral analysis regardless of sex (Table 1). For the second cohort including the behavioral assessments, mice were divided into each procedural subcohort (sham or stroke) to equalize sexes.

Stroke Modeling

Subcortical white matter stroke was performed as described [17] within the left hemisphere. Sham procedures were performed identically to the stroke but involved injection of normal saline rather than N5-iminoethyl-l-ornithine (L-Nio) (Calbiochem). All stroke or sham procedures were performed at 2 months of age, and the operator was blinded to genetic designation. Routine post-operative care was provided for 1 week to all mice. Mortality rates are presented in Table 1. Stroke lesion volume was measured using a standard estimation method for ellipses($V=\pi/6 \times$ major axislength × vertical axis length × minor axis length) in a minimum of three 40-μm tissue sections spaced 240 μm apart.

Behavioral Testing and Analysis

Behavioral testing was conducted by the Behavioral Testing Core (BTC) at UCLA using established methodology. Performance on rotarod and spontaneous alternation testing was performed serially at 7, 10, 15, and 20 weeks of age corresponding to baseline, 2 weeks, 7 weeks, and 12 weeks post-stroke. Novel object recognition and 24-h fear conditioning were performed once at 20 weeks of age. All behavioral assessments were performed in a blinded fashion. At the conclusion of the study, results were unblinded and results analyzed. Animals with missing data at any time point were excluded from the analysis. A repeated-measure two-way ANOVA with Tukey's post hoc test using alpha of 0.05 was applied for rotarod and spontaneous alternation testing. A two-way ANOVA with Tukey's post hoc test using alpha of 0.05 was applied for 24 h fear conditioning and novel objection recognition. A combined cognitive z-score was generated by averaging independent z-scores on spontaneous alternation, fear conditioning, and novel object recognition performance at 20 weeks. Data resampling was performed using MatLab 2017b with $n = 30$ and results analyzed by two-way ANOVA with Tukey's post hoc test using alpha of 0.05. Performance on all tasks was initially analyzed irrespective of sex with secondary effects of sex assessed independently.

^{18}FDG PET/CT Acquisition and Analysis

A subset of E4-TR:FAD+ transgenic mice with ($n = 4$) and without ($n = 4$) as well as E4-TR:FAD− mice with stroke (n = 4) underwent conscious tail vein injection of 37 MBq (100 μCi) ^{18}F-2-fluoro-2-deoxy-D-glucose (^{18}F-FDG). After 60 min probe uptake time, mice were anesthetized with 2% isoflurane in oxygen and placed in a dedicated imaging chamber. microPET images were acquired for 600 s (Inveon microPET, Siemens Medical Solutions USA), followed by 3D histogramming and reconstruction with a zoom factor of 2.1 using 3D-OSEM with 2 iterations followed by MAP with 18 iterations (beta = 0.1). Each microPET imaging was followed by microCT imaging (CrumpCAT [23] microCT) acquired under continuous mode using a 50-kVp 200-μA X-ray source and reconstructed using the Feldkamp algorithm. Mice were kept warm prior to and throughout the imaging procedure. Images were analyzed using AMIDE version 1.0.5 [24] imaging software. Additional analysis of regional cerebral metabolic variation between cohorts was performed essentially as described [25].

Immunohistochemistry and Immunofluoresence

At the completion of the study (5 months of age), all mice were euthanized and transcardially perfused with PBS followed by cold 4% paraformaldehyde. The brain was removed from the skull and post-fixed in 4% paraformaldehyde overnight then cryoprotected for 48 h in 30% sucrose. Cryoprotected brains were frozen on dry ice and cryosectioned in six series of 40-μm-thick floating sections. Immunofluorescence staining was performed as previously described [15]. For neuronal and microglial counts, antibody labeling was performed using the following primary antibodies: mouse anti-NeuN (Millipore Cat. No. MAB377, 1:500); goat anti-Iba-1 (Abcam Cat. No. ab5076, 1:500). Secondary antibody labeling was achieved using species-specific donkey Fab^2 antibodies. Amyloid plaque immunohistochemistry was performed as follows. Tissue sections from one series were washed in phosphate-buffered saline (PBS) for 15 min each. Endogenous peroxidase activity was blocked by incubation in 0.5% hydrogen peroxide for 30 min. Sections were rinsed in PBS, incubated in blocking buffer (2% normal goat serum, 0.3% TX-100) for 1 h, and then incubated overnight at 4 °C in DAE primary antibody (rabbit polyclonal anti-*Aβ1–13* [26]; 1:600). Sections were then rinsed in PBS and then incubated with goat anti-rabbit IgG-HRP (1:500) for 1.5 h at room temperature. After washing, sections were then incubated for 1 min 30 s in the DAB-Peroxidase Substrate Kit (Vector Laboratories, Inc.) per manufacturer protocol. Stained sections were then mounted on gelatin coated slides, dried overnight, dehydrated in serial alcohols and xylene, and coverslipped.

Thioflavin S Staining

A 0.5% solution of thioflavin S (Millipore Sigma Cat. No. T1892) was made in distilled deionized water and filtered through a 0.22-μm SFCA filter and kept shielded from light. Thioflavin S staining was carried out for 30 min at room temperature after immunostaining and mounting sections followed by dehydration as described above.

Quantification of Aβ Plaque Pathology

Quantification was performed essentially as described [27]. Briefly, examination of Aβ plaque deposition focused on coronal planes through the frontal cortex corresponding to the region of cortex containing cells with axons that project through the subcortical stroke [15] as well as coronal planes through the anterior hippocampus (3–6 per animal). Images were captured at × 5 magnification. A blinded rater used Fiji [28] to manually delineate both the left and right sensorimotor cortex as defined by anatomical landmarks [29] or the full coronal visualization of the anterior hippocampus. Left and right frontal cortex measurements were determined separately for each animal. Plaque density measured as: (1) *Aβ* staining area as percentage of total region of interest (ROI) area, (2) number of total plaques per ROI, and (3) plaque size in square millimeters was quantified and compared by genotype and injury group. Intracortical differences in amyloid staining between left and right were determined by subtracting right cortical measurements from left.

Quantification of Cell Counts and Morphology

ROIs at × 20 magnification within the sensorimotor frontal cortex overlying the subcortical stroke lesion or the corresponding region in the contralateral cortex across three serial

sections separated by 240 μm were captured under fluorescent microscopy for each animal. A blinded rater used Fiji [28] to count Neu-N-positive neurons, Iba-1+ microglia within each ROI. Counts were averaged across sections and then across animals and compared by injury group (E4-TR:FAD+ sham vs. E4-TR:FAD+ subcortical stroke). Significance testing was performed using Student's *t* test with Welch's correction. To analyze microglial morphology, we performed Sholl analysis of Iba-1-positive cells in three serial sections separated by 240 μm from a total of 14 mice animals (8 stroke/6 sham). Three regions of interest (ROIs) in the cortex overlying the white matter stroke (or sham) were imaged per section and 5 arbitrary cells per ROI were analyzed to ensure a representative sample of microglia. Using Fiji, individual microglia was selected, and a Sholl analysis was performed using a radial step size of 1.7 μm. A total of 630 microglia (45/animal) were analyzed. The mean number of intersections per step size was compared between conditions using a two-way ANOVA ($p < 0.05$) with post hoc Sidak's multiple comparisons test performed at each radial step size.

Results

Design of Novel Mouse Model of Mixed Vascular and Alzheimer's Disease

Here, we sought to develop a mouse model of mixed vascular and Alzheimer's dementia to address how white matter stroke can impact AD pathology using a relevant time scale reflecting the chronic nature of both disorders. A schematic for our implementation of this mixed vascular and Alzheimer's dementia model is shown in Fig. 1. To study the impact of white matter stroke on AD pathologic progression, we human ApoE4-TR:5XFAD transgenic mice. This strain is a cross between the 5XFAD (APP K670N/M671L (Swedish) +I716V (Florida)+V717I (London) familial Alzheimer's disease (FAD) mutations) and mutant human presenilin 1 (*PSEN1*) with the M146L+L286V FAD mutations inserted into exon 2 of the mouse *Thy1* gene) with the human ApoE4 knock-in mouse line as described in the "Methods." Mice were bred homozygous for the human ApoE4 knock-in allele and hemizygous for the FAD transgene using females as the carrier (Supplemental Fig. 1). A subcortical white matter stroke or sham procedure is introduced at 2 months of age prior to the development of significant AD pathology. Following stroke induction, we measured brain metabolism, motor and cognitive performance, and tissue pathology at 5 months of age to determine if antecedent white matter stroke accelerates (Fig. 1, small dashed line) or decelerates the progression of AD (Fig. 1, large dashed line). The enrollment of individual animals with sex, genotype, experimental condition, and mortality are presented in Table 1.

Subcortical Stroke in Human ApoE4-TR:5XFAD Transgenic Mice

Seven days after stroke induction in human ApoE40-TR:5XFAD transgenic mice, we determined if the 5XFAD transgene had an effect on the stroke lesion and cellular changes within the peri-infarct white matter. As previously reported, this ischemic lesion produced a focal loss of myelin and axons within the subcortical white matter beneath sensorimotor cortex (Fig. 2). Elliptical stroke lesion volume was measured in E4-TR:FAD- and E4-TR:FAD+ animals. There was no effect ofthe FAD transgene on subcortical stroke lesion size(4819 ± 1067 vs. 6867 ± 601.4 μm^3; $p = 0.094$, $n = 5$ E4-TR:FAD−, $n = 9$ E4-TR:FAD+). Subcortical stroke produces a dense loss of oligodendrocytes within the white matter (Fig. 2c) and a robust reactive astrocytosis (Fig. 2d) that was not significantly

different between E4-TR:FAD+ and E4-TR:FAD− mice. Sham procedures produced no identifiable abnormality in subcortical white matter.

Frontal Cortex Amyloid Deposition

hApoE4-TR:5XFAD transgenic mice underwent a sham procedure or subcortical stroke at 2 months of age and allowed to undergo amyloid plaque accumulation until 5 months of age. Figure 3a demonstrates the pattern of frontal cortex diffuse amyloid staining observed at 5 months in the E4-TR:FAD+ mice with sham (left) or stroke (right).Localization of stroke is restricted to the subcortical white matter underlying the frontal sensorimotor cortex (arrow, Fig. 3a). In the area of left frontal sensorimotor cortex (Supplemental Fig. 2) immediately overlying the subcortical white matter stroke (arrow, Fig. 3b, right panel) amyloid plaque staining in the E4-TR:FAD+ with stroke group was reduced compared with sham-treated mice at 5 months of age (Fig. 3b, left). In sham-treated E4-TR:FAD+ mice, there was no difference in the amount of diffuse amyloid staining (per unit area) detected between left and right hemispheres (mean difference, +0.11), while in E4-TR:FAD+ mice with a subcortical stroke, the difference between left and right amyloid staining was significantly reduced (mean difference, −0.79, p= 0.043 by Mann-Whitney U test, n = 8 E4-TR:FAD−, n = 9 E4-TR:FAD+) (Fig. 3c). Examination of the interhemispheric difference in plaque number showed a similar decrease in the stroke-affected hemisphere, though non-significant (7.14 vs. −95.33; p=0.20). Further examination of amyloid plaque morphology suggested that in E4-TR:FAD+ mice with subcortical white matter stroke, amyloid plaque size was smaller than in E4-TR:FAD+ sham-treated mice (Fig. 3b, bottom). To quantify this, we binned frontal cortex plaque size by area (by 1 μm^2 for the first 5 μm^2 and then by 5 up to 80 μm^2) across all treated animals and compared the average number of plaques per size per bin between E4-TR:FAD+ sham mice (red circles) and E4-TR:FAD+ stroke mice (blue squares). Chi-squared analysis of these plaque size distributions indicates that in E4-TR:FAD+ stroke mice, plaque size was shifted significantly towards a smaller size (p<0.0001, Chi-square 293.7, df=19) (Fig. 3d). To control for the possibility that subcortical white matter stroke resulted in neuronal loss in overlying cortex, we quantified the number of NeuN-positive neurons (per unit area) in the overlying cortex in E4-TR:FAD+ sham and E4-TR:FAD+ stroke mice with no difference in the number of surviving neurons within the overlying frontal cortex (60.2 ± 3.58 vs. 60.37 ± 4.52, p = 0.72; Supplemental Fig. 3) suggesting that the observed differences in frontal cortex amyloid did not result from decreased Thy1-FAD transgene expression due to neuronal cell death after stroke. We also examined the effect of stroke on amyloid deposition in the hippocampus. Anatomically matched sections of hippocampus from E4-TR:FAD+ sham or E4-TR:FAD+ stroke mice at 5 months of age were immunostained for diffuse amyloid. Marked variability in hippocampal plaque deposition was notable in both conditions and at this age, most of the amyloid deposition was notable in the CA1 region of the hippocampus in both E4-TR:FAD+ sham (Supplemental Fig. 4a) and E4-TR:FAD+ stroke mice (Supplemental Fig. 4b). Higher magnification images demonstrate similar plaque size in both E4-TR:FAD+ sham (Supplemental Fig. 4a, bottom) and E4-TR:FAD+ stroke mice (Supplemental Fig. 4b, bottom). There were no significant differences in amyloid-positive hippocampal area between sham and stroke E4-TR:FAD+ mice (0.301 ± 0.108 vs. 0.570 ± 0.336; p=0.48) (Supplemental Fig. 4c) nor hippocampal plaque number (52.25 ± 14.33 vs. 80.5 ± 35.83; p = 0.49) (Supplemental Fig. 4d).

Changes in Brain Metabolism

To further confirm if our observation of reduced cortical amyloid after subcortical white matter stroke was secondary to reduced cortical activity after stroke, we performed ^{18}FDG-PET/CT in a subset of mice. As previously noted [25], mouse brain glucose metabolism is highly variable and therefore, we used a proportional scaling approach to normalize each animal's FDG signal to the whole brain. After this normalization, we compared regional variation in FDG uptake between various brain regions (Supplemental Fig. 5). This voxel-based analysis revealed several focal regions of increased FDG uptake in E4-TR:FAD+ mice with stroke compared with sham (AD) including the thalamus. Decreased FDG uptake in E4-TR:FAD+ mice with stroke compared with sham (AD) was noted only in the focal region of the stroke lesion as could be expected. Comparing just the M1/S1 region of cortex where reduced amyloid was noted (Fig. 3), we found no significance difference between FDG uptake inE4-TR:FAD+ animals with stroke compared with sham (or to stroke alone in E4-TR:FAD− mice, $n = 4$/group), indicating that reduced cortical amyloid after stroke was not secondary to reduced cortical activity.

Motor and Cognitive Performance

To determine the effect of mixed vascular and AD modeling on motor performance after stroke, we utilized serial rotarod testing on four groups of mice: sham (E4-TR:FAD−), stroke (E4-TR:FAD−), AD (E4-TR:FAD+), and AD+stroke (E4-TR:FAD+) beginning at 2 weeks post-procedure and continuing every 5 weeks until 20 weeks of age (Fig. 4a). The AD group (pink; E4-TR:FAD+) showed a minor and stable percent change from baseline in latency to fall (s) (Fig. 4a) as expected after only a sham subcortical injection. The stroke group (blue; E4-TR:FAD-) demonstrated a progressive decline in latency to fall over time. In the combined stroke and AD model (red; E4-TR:FAD+ with stroke), motor performance initially mirrored the stroke group but improved over time. Due to significant intra-group variability in latency to fall, repeated measures two-way ANOVA revealed a significant effect of time ($p = 0.0056$, $F = 5.745$, $df = 52$) on rotarod performance predominantly after stroke but did not demonstrate significant differences in rotarod performance between stroke, AD, and AD+stroke ($p = 0.23$). This is not surprising given the minor and transient forelimb deficit resulting from a small subcortical white matter stroke.

To determine the effect of AD, stroke and combined pathologies on cognitive performance, we utilized multiple tasks of working memory and executive function that have previously been validated in the original EFAD mouse model including spontaneous alternation (Y-maze), fear conditioning, and novel object recognition [19, 30]. Serial performance on spontaneous alternation were assessed prior to stroke or sham procedures and repeatedly measured every 5 weeks (Fig. 4b). Rates of spontaneous alternation were not significantly affected by either genotype or stroke procedure. At 20 weeks of age, freezing time (s) in a 24-h fear-conditioning task (Fig. 4c) demonstrated a significant effect of treatment group ($p = 0.0003$ by two-way ANOVA, $F = 11.88$, $df = 15$) with both stroke ($p = 0.0133$) and AD ($p = 0.0002$) demonstrating a significant decrease in recall of the noxious stimulus compared with sham controls. The AD+stroke group demonstrated a significant increase in recall compared with AD ($p = 0.0085$) and performed approximately at the level of stroke animals. As a global measure of cognitive performance, we generated an average cognitive

z-score measure using each animal's performance on spontaneous alternation at 20 weeks (% alternation), novel object recognition (time with novel object), and freezing time (sec) on the 24-h fear-conditioning task (Fig. 4d). This global cognitive measure suggested a trend ($p = 0.124$ by two-way ANOVA, $F = 2.46$, $df = 44$) towards improved cognitive performance in the combined AD and stroke model. Data resampling based on the distribution of observed z-scores using an $n = 30$ demonstrated a significant effect of treatment ($p < 0.0001$ by two-way ANOVA, $F = 45.85$, $df = 116$). In the bootstrapped data sample, stroke resulted in a significant cognitive impairment (adjusted $p = 0.0017$), as did AD (adjusted $p < 0.0001$), while in the AD+stroke group, there was a significant improvement in cognitive function compared with AD (adjusted $p < 0.0001$). Subgroup analysis of fear conditioning and novel objection recognition tasks are presented in Supplemental Figs. 6 and 7, respectively.

Microglial Response

Based on the observed reduction in cortical amyloid seen in the combined AD and stroke model that occurred in the absence of changes in cortical metabolic activity or neuronal cell death after stroke, we reasoned that this reduction in amyloid burden could be accounted for by changes in microglial number or morphology triggered by stroke. We labeled sections of frontal cortex for Iba-1(+) cells (Fig. 5). In the region of cortex overlying the subcortical stroke (St) where amyloid staining was reduced after stroke (Fig. 5a, b), E4-TR:FAD+ sham mice display a frequent and even distribution of Iba-1(+) cells (Fig. 5c). In E4-TR:FAD+ mice with stroke, the frequency of Iba-1(+) cells were increased and clustered in a pattern that was not observed in E4-TR:FAD+ sham mice (Fig. 5d). ThioS (+) plaques in E4-TR:FAD+ stroke mice were more often associated with clusters of Iba-1(+) microglia compared with sham (Fig. 4e, f). Quantification of the number of Iba-1(+) cells within the cortex demonstrated a significant increase between E4-TR:FAD+ sham and E4-TR:FAD+ stroke mice (Fig. 5; $p = 0.044$, $n = 6$ E4-TR:FAD−, $n = 8$ E4-TR:FAD+). Analysis of microglial cellular morphology indicated greater branching morphology in the stroke-injured AD animals compared with sham ($p < 0.0001$ by two-way ANOVA, $F = 32.09$, $df = 96$) (Fig. 5h). Significant differences were noted at individual cellular radii between 5.1 and 10.2 μm ($p < 0.05$) consistent with increased branching morphology of cortical microglia.

Discussion

Given the increasing recognition that few cases of dementia result solely from the classic Alzheimer's disease plaque and tangle pathology, there is an urgent need to develop basic science models that more accurately reflect the pathology seen in human patients. The interaction between subcortical white matter ischemia and AD is an area deserving of increased focus [5], as highlighted by the NIH Alzheimer's Disease-Related Dementias Summit in 2016 [31]. Here, we establish a new paradigm for studying the overlap between subcortical white matter ischemia and AD using a versatile and well-characterized mouse model of white matter stroke. This focal white matter stroke model can be easily combined with any number of existing AD transgenic models regardless of their focus on amyloidogenesis or tauopathy. This stroke lesion shares a number of features with human lacunar infarctions including focal axonal loss, gliosis, and minor functional deficits [16, 32, 33]. The local injury response within the white matter was not different in the

presence of the 5XFAD transgene suggesting it has no influence on axonal vulnerability to ischemia. However, this subcortical lesion also impacts the cortical neurons whose axons are damaged [15, 17], providing a clear rationale for examining the effect of subcortical stroke on pathologic changes in the overlying frontal cortex (Fig. 6).

The present data suggest that a subcortical white matter ischemic lesion prior to the onset of amyloid accumulation in human ApoE4-TR:5XFAD transgenic mice exerts a delayed effect on the connected cortex. This subcortical injury modifies cortical amyloid accumulation independent of neurodegeneration. Rather, subcortical stroke appears to promote a unique microglial response in the cortex that helps to reduce amyloid burden, presumably through enhanced clearance. Evaluations of motor and cognitive performance in this mixed vascular and AD model of dementia produced variable results generally supportive of our pathologic observations of reduced amyloid and with trends towards improved motor and cognitive performance after stroke. This initial approach at developing an animal model to better represent both the chronicity and co-morbid neuropathologies seen in humans with dementia should lay the foundation for improving our understanding of the fundamental biology present in the majority of dementia cases.

With increasing recognition of the overlap between AD and subcortical white matter changes, other approaches to model mixed dementia have examined various features of this multiple injury paradigm. In the early phase after a MCAO or focal cortical stroke, thioflavin S detection of amyloid plaques are transiently increased in APPswe/PS1dE9 mice [14]. Notably, this effect was highly transient with normalization of plaque burden by 14 days, suggesting that despite the transient increase in amyloid generation resulting from ischemia, amyloid clearance mechanisms are activated by stroke. In hypertensive rats, distal MCAO is associated with increases in beta-amyloid deposition inthe thalamus at 14 days post-stroke [34]. Increases in Aβ oligomers are also found early on in the thalamus after distal MCAO [35], indicating that direct neuronal ischemia does increase amyloid production by neurons. Modeling of the more common co-morbid dementia pathology of subcortical ischemic lesions that lack direct neuronal ischemia is less studied. Anticipating worsening pathology, Whitehead et al. [36] introduced striatal ischemia with endothelin-1 and co-injected Aβ fragments. This artificial modeling approach resulted in an enhanced inflammatory response but again only early time points (7–14 days) after stroke were assessed. In a similar modeling approach and consistent with the results presented here, microglial ramification was increased in the cortex of the co-morbid Aβ and endothelin-1-injected rats [37], suggesting that comorbid amyloid and ischemic injuries interact to promote inflammation in the cortex. To our knowledge, the approach presented here is the first animal model of mixed vascular and AD dementia that models both subcortical white matter ischemia using a FAD transgenic mouse strain and employs a more chronic time scale. Given the chronicity of both AD and subcortical white matter ischemic lesions, models of mixed dementia should focus on these extended time points. A limitation of this modeling approach using an early subcortical white matter stroke lesion is that in younger animals, this may have a priming effect on the immune system that would be blunted as animals age. Using this model, the timing of stroke modeling and AD-associated pathologies can be adjusted as needed based upon the AD model, its rate of progression, and the presence of additional desired features such as age or gender effects.

In this study, the behavioral assessments of motor function and cognition produced variable results. Several cognitive tasks demonstrated significant variation based on sex, consistent with prior reports in the original EFAD line [30]. In this human ApoE4-TR:5XFAD transgenic strain with a reduced influence of the SJL background present in the original EFAD strain, we observed opposite results from those reported, with E4-TR:FAD+ male mice demonstrating more robust and reliable cognitive impairment than E4-TR:FAD+ female mice even in the absence of stroke. Despite this blunted E4-TR:FAD+ genotype effect in female mice, our finding of reduced cortical amyloid pathology in the mixed model is supported by global z-score assessments of cognitive performance using mice of both sexes. Motor performance in the mixed AD and stroke model showed a non-significant trend that supported our pathologic observation of reduced amyloid burden in sensorimotor cortex. In this subcortical stroke model, motor function is difficult to measure accurately with younger animals as they show a rapid recovery [33] and the rotarod task may not be sensitive enough to detect subtle changes in forelimb function. In addition, the ApoE4 genotype blunted the previously noted early recovery suggesting E4-independent effects on recovery after stroke, similar to those that have been reported in humans [38]. Overall, the motor and cognitive performance of human ApoE4-TR:5XFAD transgenic mice with stroke indicates that the assumption that two co-morbid pathologies must worsen brain function may not be true.

In E4-TR:FAD+ mice with stroke, we observed a significant decrease in ipsilateral cortical amyloid associated with a reduction in plaque size. As we showed and as has been documented in the original EFAD mouse model, there is minimal neuronal cell death at 6 months despite significant amyloid plaque accumulation [19]. The connectivity of cortical brain regions has been suggested as a central feature dictating amyloid plaque burden [39–41]. In this stroke model designed to mimic a lacunar stroke [16], the majority of stroke-injured axons project from neurons in overlying sensorimotor cortex [17, 32], supporting the influence of cortical connectivity on amyloid accumulation. Increases in neuronal activity promote amyloidogenesis in specific cortical regions [42]. We have previously demonstrated that subcortical ischemic stroke reduces the length of the axon initial segment (AIS) and the number of axoaxonic synapses in neurons damaged by the stroke [15]. These changes in AIS length and synaptic connections are likely to limit neuronal excitability in stroke-injured neurons, suggesting that reduced neuronal activity after stroke could explain the reduced amyloid burden we observed here.

An alternative hypothesis for reduced cortical amyloid in this mixed dementia model using human ApoE4-TR:5XFAD transgenic mice is that amyloid clearance mechanisms are accelerated by stroke. This could occur through several mechanisms including stroke-induced opening of the blood-brain barrier or activation of neuronal-microglial signaling mechanisms. This stroke model opens the blood-brain barrier locally in the white matter [43], but this is not likely to affect the overlying cortex. The interaction between neurons and microglia in AD is increasingly recognized [44], though the interaction is complex with microglia playing an important role in amyloid clearance [45, 46] but also contributing to neuronal loss [47]. Recent single cell RNA-seq approaches to deeply characterize microglial phenotypes during neurodegeneration indicates that these cells change their response profile over time moving from a type I interferon response early on to a type II interferon profile

later in disease [48]. In part, this transition may be triggered by proximity to injured neurons. Retrograde axonal injury signals are conveyed back to neurons [49] and though for cortical neurons these precise molecular signals are just beginning to emerge [50], they may function to flag injured cortical neurons, activate microglia and lead to synaptic pruning.

On an AD genetic background, cortical microglia stimulated by stroke may turn their attention to clearing Aβ. We hypothesize that this is the predominant mechanism responsible for the findings reported here, with an increased number and clustered pattern of microglia around thioflavin S-positive plaques in E4-TR:FAD+ mice with stroke. Such enhanced clustering may be driven by the E4 allele [51], though in this study all mice wereE4+ and therefore the enhanced microglial response is driven by stroke alone. In a broader context, the aging brain at risk for dementia likely exists in a constant continuum of stimuli that promote and reduce amyloid burden. Here, we show that in a pro-AD pathology environment, an early subcortical injury pushes the brain towards a reduced amyloid burden.

The high degree of co-morbid AD and cerebrovascular pathologies seen in humans has complicated therapeutic strategies designed to reduce amyloid burden. While many reasons for this translation failure exist, animal modeling of mixed AD and vascular dementia that is relevant to the co-morbid pathologies is essential to understand the neurobiology and design the next generation of dementia therapeutics.

Supplementary Material

Refer to Web version on PubMed Central for supplementary material.

Acknowledgments

Behavioral experiments were conducted in the UCLA Behavior Testing Core under the supervision of Drs. Jesse Cushman, Abha Karki Rajbhandari and conducted by Irina Zhuravka.

Funding

This study was funded by NINDS NS083740 (JDH), the American Federation for Aging Research/Rosalind and Arthur Gilbert Foundation New Investigator in Alzheimer’s disease award (JDH), the National Center for Advancing Translational Sciences UCLA CTSI Grant UL1TR000124, the Brain Research Institute, the American Heart Association Undergraduate Student Research Program (JMH), and generous gifts from the Paul Slavik Foundation, The Sam and Ida Turken Charitable Foundation (EYH), and support from the UCLA Department of Neurology.

References

1. Attems J, Jellinger KA. The overlap between vascular disease and Alzheimer’s disease—lessons from pathology. BMC Med. 2014;12:206. [PubMed: 25385447]
2. Erten-Lyons D, Woltjer R, Kaye J, Mattek N, Dodge HH, Green S, et al. Neuropathologic basis of white matter hyperintensity accumulation with advanced age. Neurology. 2013;81(11):977–83. [PubMed: 23935177]
3. Gouw AA, van der Flier WM, Fazekas F, van Straaten EC, Pantoni L, Poggesi A, et al. Progression of white matter hyperintensities and incidence of new lacunes over a 3-year period: the Leukoaraiosis and disability study. Stroke. 2008;39(5):1414–20. [PubMed: 18323505]
4. Benavente OR, Hart RG, McClure LA, Szychowski JM, Coffey CS, Pearce LA. Effects of clopidogrel added to aspirin in patients with recent lacunar stroke. N Engl J Med. 2012;367(9):817–25. [PubMed: 22931315]

5. Lee S, Viqar F, Zimmerman ME, Narkhede A, Tosto G, Benzinger TL, et al. White matter hyperintensities are a core feature of Alzheimer's disease: evidence from the dominantly inherited Alzheimer network. Ann Neurol. 2016;79(6):929–39. [PubMed: 27016429]
6. Ringman JM, Monsell S, Ng DW, Zhou Y, Nguyen A, Coppola G, et al. Neuropathology of autosomal dominant Alzheimer disease in the National Alzheimer Coordinating Center Database. J Neuropathol Exp Neurol. 2016;75(3):284–90. [PubMed: 26888304]
7. Brenowitz WD, Hubbard RA, Keene CD, Hawes SE, Longstreth WT Jr, Woltjer RL, et al. Mixed neuropathologies and associations with domain-specific cognitive decline. Neurology. 2017;89(17):1773–81. [PubMed: 28939667]
8. Rosenberg GA. Inflammation and white matter damage in vascular cognitive impairment. Stroke. 2009;40(3 Suppl):S20–3. [PubMed: 19064797]
9. Zlokovic BV. Cerebrovascular effects of apolipoprotein E: implications for Alzheimer disease. JAMA Neurol 2013;70(4):440–4, 444. [PubMed: 23400708]
10. Kanekiyo T, Liu CC, Shinohara M, Li J, Bu G. LRP1 in brain vascular smooth muscle cells mediates local clearance of Alzheimer's amyloid-beta. J Neurosci. 2012;32(46):16458–65.
11. Nikolaev A, McLaughlin T, O'Leary DD, Tessier-Lavigne M. APP binds DR6 to trigger axon pruning and neuron death via distinct caspases. Nature. 2009;457(7232):981–9. [PubMed: 19225519]
12. Amtul Z, Nikolova S, Gao L, Keeley RJ, Bechberger JF, Fisher AL, et al. Comorbid Abeta toxicity and stroke: hippocampal atrophy, pathology, and cognitive deficit. Neurobiol Aging. 2014;35(7):1605–14. [PubMed: 24491422]
13. Sarajarvi T, Lipsanen A, Makinen P, Peraniemi S, Soininen H, Haapasalo A, et al. Bepridil decreases Abeta and calcium levels in the thalamus after middle cerebral artery occlusion in rats. J Cell Mol Med. 2012;16(11):2754–67. [PubMed: 22805236]
14. Garcia-Alloza M, Gregory J, Kuchibhotla KV, Fine S, Wei Y, Ayata C, et al. Cerebrovascular lesions induce transient beta-amyloid deposition. Brain. 2011;134(Pt 12):3697–707. [PubMed: 22120142]
15. Hinman JD, Rasband MN, Carmichael ST. Remodeling of the axon initial segment after focal cortical and white matter stroke. Stroke. 2013;44(1):182–9. [PubMed: 23233385]
16. Sozmen EG, Hinman JD, Carmichael ST. Models that matter: white matter stroke models. Neurotherapeutics. 2012;9(2):349–58. [PubMed: 22362423]
17. Nunez S, Doroudchi MM, Gleichman AJ, Ng KL, Llorente IL, Sozmen EG, et al. A versatile murine model of subcortical white matter stroke for the study of axonal degeneration and white matter neurobiology. J Vis Exp. 2016;(109). 10.3791/53404.
18. Hayden EY, Putman J, Nunez S, Shin WS, Oberoi M, Charreton M, et al. Ischemic axonal injury up-regulates MARK4 in cortical neurons and primes tau phosphorylation and aggregation. Acta Neuropathol Commun. 2019;7(1):135. [PubMed: 31429800]
19. Youmans KL, Tai LM, Nwabuisi-Heath E, Jungbauer L, Kanekiyo T, Gan M, et al. APOE4-specific changes in Abeta accumulation in a new transgenic mouse model of Alzheimer disease. J Biol Chem. 2012;287(50):41774–86.
20. Sullivan PM, Mezdour H, Aratani Y, Knouff C, Najib J, Reddick RL, et al. Targeted replacement of the mouse apolipoprotein E gene with the common human APOE3 allele enhances diet-induced hypercholesterolemia and atherosclerosis. J Biol Chem. 1997;272(29):17972–80.
21. Oakley H, Cole SL, Logan S, Maus E, Shao P, Craft J, et al. Intraneuronal beta-amyloid aggregates, neurodegeneration, and neuron loss in transgenic mice with five familial Alzheimer's disease mutations: potential factors in amyloid plaque formation. J Neurosci. 2006;26(40):10129–40.
22. Zhong L, Xie YZ, Cao TT, Wang Z, Wang T, Li X, et al. A rapid and cost-effective method for genotyping apolipoprotein E gene polymorphism. Mol Neurodegener. 2016;11:2. [PubMed: 26754117]
23. Taschereau R, Vu N, Chatziioannou AF. Calibration and data standardization of a prototype bench-top preclinical CT. Nuclear Science Symposium and Medical Imaging Conference. Seattle. Washington, USA: IEEE; 2014.

24. Loening AM, Gambhir SS. AMIDE: a free software tool for multimodality medical image analysis. Mol Imaging. 2003;2(3):131–7. [PubMed: 14649056]
25. Welch A, Mingarelli M, Riedel G, Platt B. Mapping changes in mouse brain metabolism with PET/CT. J Nucl Med. 2013;54(11):1946–53. [PubMed: 24009277]
26. Lim GP, Chu T, Yang F, Beech W, Frautschy SA, Cole GM. The curry spice curcumin reduces oxidative damage and amyloid pathology in an Alzheimer transgenic mouse. J Neurosci. 2001;21(21):8370–7. [PubMed: 11606625]
27. Grant DA, Serpa R, Moattari CR, Brown A, Greco T, Prins ML, et al. Repeat mild traumatic brain injury in adolescent rats increases subsequent beta-amyloid pathogenesis. J Neurotrauma. 2018;35(1): 94–104. 10.1089/neu.2017.5042. [PubMed: 28728464]
28. Schindelin J, Arganda-Carreras I, Frise E, Kaynig V, Longair M, Pietzsch T, et al. Fiji: an open-source platform for biological-image analysis. Nat Methods. 2012;9(7):676–82. [PubMed: 22743772]
29. Paxinos G, Franklin KB. The mouse brain in stereotactic coordinates. 2nd ed. San Diego: Academic Press; 2001.
30. Tai LM, Balu D, Avila-Munoz E, Abdullah L, Thomas R, Collins N, et al. EFAD transgenic mice as a human APOE relevant preclinical model of Alzheimer's disease. J Lipid Res. 2017;58(9):1733–55. [PubMed: 28389477]
31. Corriveau RA, Koroshetz WJ, Gladman JT, Jeon S, Babcock D, Bennett DA, et al. Alzheimer's Disease-Related Dementias Summit 2016: national research priorities. Neurology. 2017;89(23):2381–91. [PubMed: 29117955]
32. Sozmen EG, Kolekar A, Havton LA, Carmichael ST. A white matter stroke model in the mouse: axonal damage, progenitor responses and MRI correlates. J Neurosci Methods. 2009;180(2):261–72. [PubMed: 19439360]
33. Rosenzweig S, Carmichael ST. Age-dependent exacerbation of white matter stroke outcomes: a role for oxidative damage and inflammatory mediators. Stroke. 2013;44(9):2579–86. [PubMed: 23868277]
34. Zhang J, Zhang Y, Li J, Xing S, Li C, Li Y, et al. Autophagosomes accumulation is associated with beta-amyloid deposits and secondary damage in the thalamus after focal cortical infarction in hypertensive rats. J Neurochem. 2012;120(4):564–73. [PubMed: 21950964]
35. Ong LK, Zhao Z, Kluge M, Walker FR, Nilsson M. Chronic stress exposure following photothrombotic stroke is associated with increased levels of amyloid beta accumulation and altered oligomerisation at sites of thalamic secondary neurodegeneration in mice. J Cereb Blood Flow Metab. 2017;37(4):1338–48. [PubMed: 27342322]
36. Whitehead SN, Hachinski VC, Cechetto DF. Interaction between a rat model of cerebral ischemia and beta-amyloid toxicity: inflammatory responses. Stroke. 2005;36(1):107–12. [PubMed: 15591213]
37. Amtul Z, Whitehead SN, Keeley RJ, Bechberger J, Fisher AL, McDonald RJ, et al. Comorbid rat model of ischemia and beta-amyloid toxicity: striatal and cortical degeneration. Brain Pathol. 2015;25(1):24–32. [PubMed: 24725245]
38. Cramer SC, Procaccio V, Americas G, Investigators GIS. Correlation between genetic polymorphisms and stroke recovery:analysis of the GAIN Americas and GAIN international studies. Eur J Neurol. 2012;19(5):718–24. [PubMed: 22221491]
39. Prescott JW, Guidon A, Doraiswamy PM, Roy Choudhury K, Liu C, Petrella JR, et al. The Alzheimer structural connectome: changes in cortical network topology with increased amyloid plaque burden. Radiology. 2014;273(1):175–84. [PubMed: 24865310]
40. Lim HK, Nebes R, Snitz B, Cohen A, Mathis C, Price J, et al. Regional amyloid burden and intrinsic connectivity networks in cognitively normal elderly subjects. Brain. 2014;137(Pt 12):3327–38. [PubMed: 25266592]
41. Sepulcre J, Grothe MJ, Sabuncu M, Chhatwal J, Schultz AP, Hanseeuw B, et al. Hierarchical organization of tau and amyloid deposits in the cerebral cortex. JAMA Neurol. 2017;74(7):813–20. [PubMed: 28558094]

42. Bero AW, Yan P, Roh JH, Cirrito JR, Stewart FR, Raichle ME, et al. Neuronal activity regulates the regional vulnerability to amyloid-beta deposition. Nat Neurosci. 2011;14(6):750–6. [PubMed: 21532579]
43. Sozmen EG, Rosenzweig S, Llorente IL, DiTullio DJ, Machnicki M, Vinters HV, et al. Nogo receptor blockade overcomes remyelination failure after white matter stroke and stimulates functional recovery in aged mice. Proc Natl Acad Sci U S A. 2016;113(52):E8453–E62.
44. Hansen DV, Hanson JE, Sheng M. Microglia in Alzheimer's disease. J Cell Biol. 2018;217(2):459–72. 10.1083/jcb.201709069. [PubMed: 29196460]
45. Tahara K, Kim HD, Jin JJ, Maxwell JA, Li L, Fukuchi K. Role of toll-like receptor signalling in Abeta uptake and clearance. Brain. 2006;129(Pt 11):3006–19. [PubMed: 16984903]
46. Zhao R, Hu W, Tsai J, Li W, Gan WB. Microglia limit the expansion of beta-amyloid plaques in a mouse model of Alzheimer's disease. Mol Neurodegener. 2017;12(1):47. [PubMed: 28606182]
47. Spangenberg EE, Lee RJ, Najafi AR, Rice RA, Elmore MR, Blurton-Jones M, et al. Eliminating microglia in Alzheimer's mice prevents neuronal loss without modulating amyloid-beta pathology. Brain. 2016;139(Pt 4):1265–81. [PubMed: 26921617]
48. Mathys H, Adaikkan C, Gao F, Young JZ, Manet E, Hemberg M, et al. Temporal tracking of microglia activation in neurodegeneration at single-cell resolution. Cell Rep. 2017;21(2):366–80. [PubMed: 29020624]
49. Hinman JD. The back and forth of axonal injury and repair after stroke. Curr Opin Neurol. 2014;27(6):615–23. [PubMed: 25364952]
50. Joy MT, Ben Assayag E, Shabashov-Stone D, Liraz-Zaltsman S, Mazzitelli J, Arenas M, et al. CCR5 is a therapeutic target for recovery after stroke and traumatic brain injury. Cell. 2019;176(5):1143–57 e13.
51. Rodriguez GA, Tai LM, LaDu MJ, Rebeck GW. Human APOE4 increases microglia reactivity at Abeta plaques in a mouse model of Abeta deposition. J Neuroinflammation. 2014;11:111. [PubMed: 24948358]

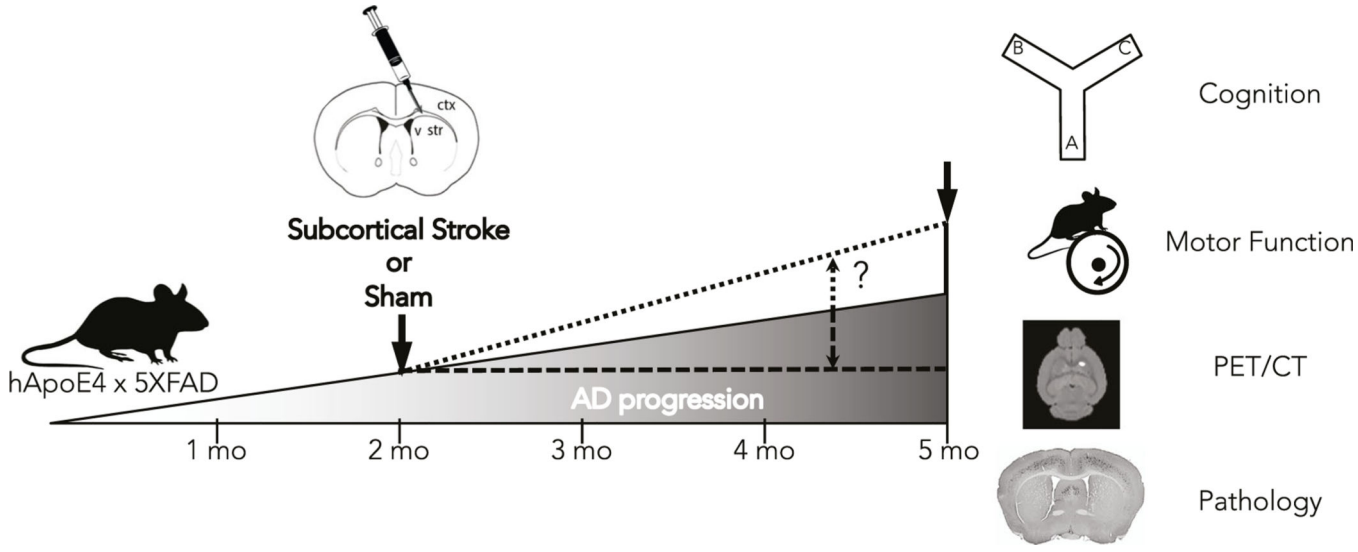

Fig. 1.

Schematic of a novel model of combined subcortical stroke and AD. Human ApoE4-TR:5XFAD transgenic mice were subjected to an early (2 months) subcortical stroke or sham procedure. Mice were tracked over 3 months with serial motor and cognitive tasks, PET/CT, and pathological assessments to determine whether an early subcortical stroke can promote (small dashed line) or reduce (large dashed line) the progression of AD hallmarks

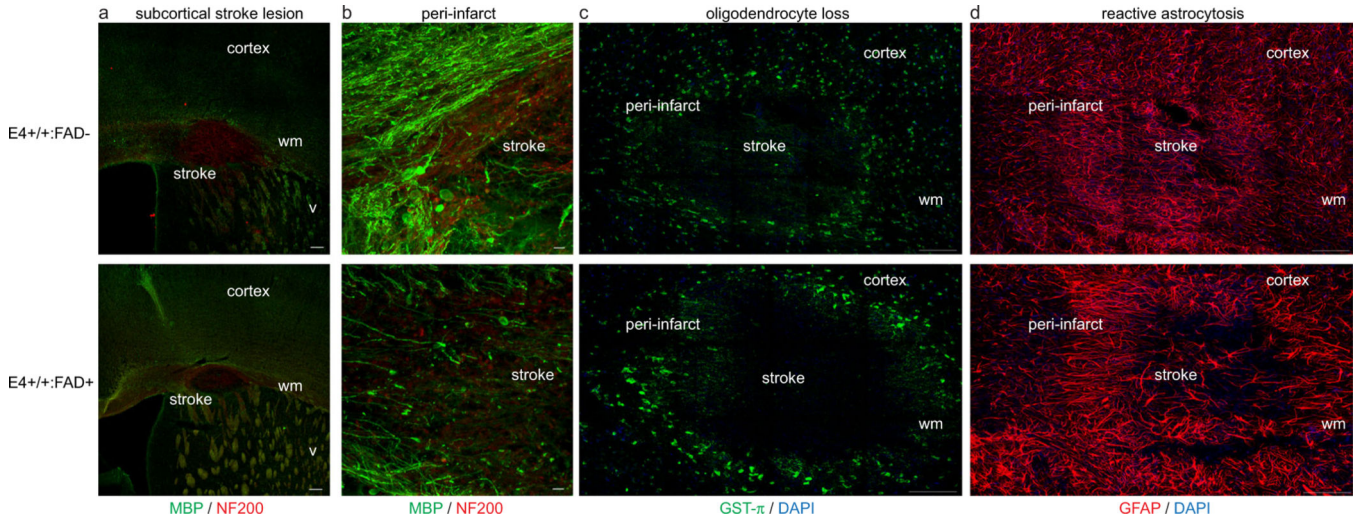

Fig. 2.

Subcortical stroke in human ApoE4-TR:5XFAD transgenic mice. Immunolabeling for myelin basic protein (green) and neurofilament-200 (NF200, red) at 7 days after stroke demonstrates a similar size-targeted ischemic lesion in the subcortical white matter in both E4-TR:FAD- (top) and E4-TR:FAD+ (bottom) animals (**a**). Dense loss of myelin and axonal swellings are present within the stroke core and peri-infarct white matter (**b**). No difference was observed in oligodendrocyte loss (**c**) or reactive astrocytosis (**d**) comparing stroke lesions in E4-TR:FAD- (top) and E4-TR:FAD+ (bottom) animals. Scale bars = 200 μm (**a**), 50 μm (**b**), 100 μm (**c**, **d**); wm, white matter; v, ventricle

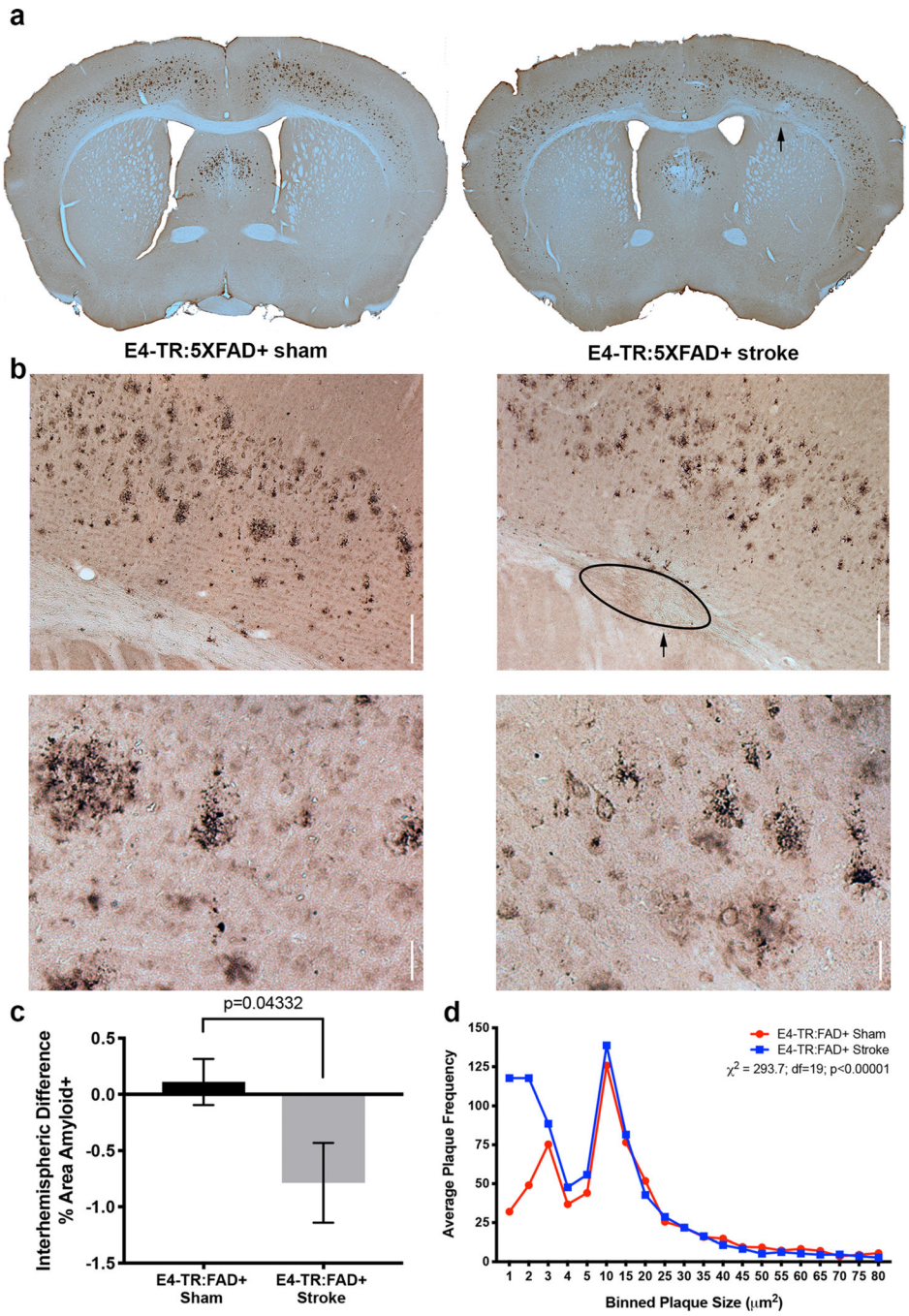

Fig. 3.

Subcortical stroke reduces cortical amyloid accumulation. Three months after sham or subcortical stroke (arrow), amyloid accumulation in the frontal cortex of E4-TR:FAD+ mice was determined (**a**). Compared with sham, labeling of the frontal cortex for Aβ demonstrates a reduction in amyloid within the cortex overlying the subcortical stroke (**b**, top). Higher-magnification images indicate a reduction in plaque size in the stroke-injured animals compared with sham (**b**, bottom). Quantification of the interhemispheric difference in percent area of amyloid staining within sensorimotor cortex between sham and stroke (**c**;

$p = 0.043$, $n = 8$ E4-TR:FAD+ sham, 9 E4-TR:FAD+ stroke). Distribution of average plaque size between sham (red circles) and stroke (blue squares) indicates a significant shift towards smaller plaque size in animals with a subcortical stroke (**d**; $p < 0.0001$ by Chi-square). Scale bars = 100 μm

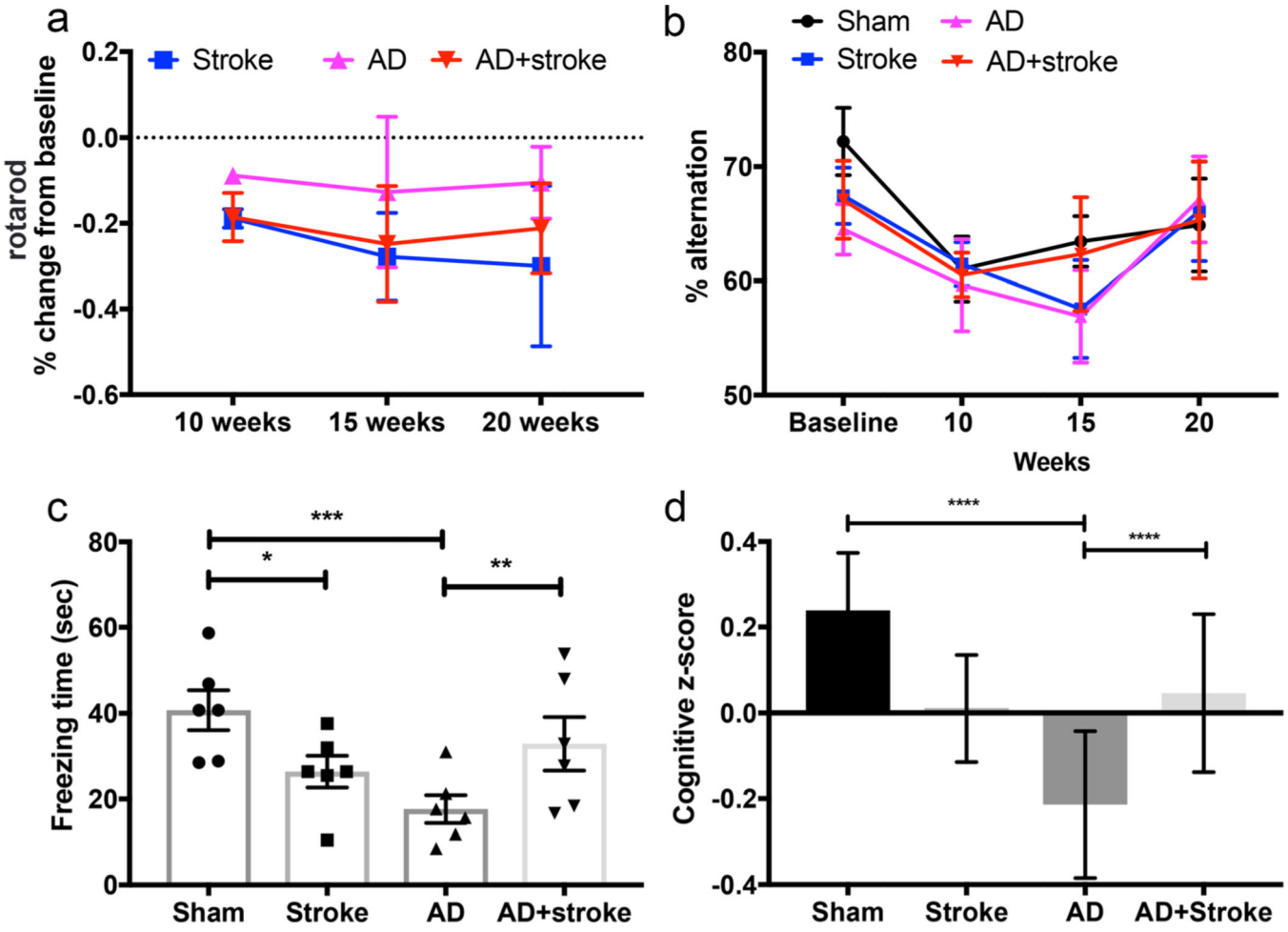

Fig. 4.

Behavioral assessment of combined subcortical stroke and AD modeling. Serial assessments of latency to fall (s) on rotarod testing measured over time shown as percent change from baseline testing (**a**). E4-TR:FAD+ mice (AD, pink) show a stable and minor change from baseline over time while E4-TR:FAD- mice with stroke (stroke, blue) show a progressive motor deficit. E4-TR:FAD+ mice with stroke (AD+stroke, red) show a similar initial motor deficit that improves over time, though not statistically significant from stroke alone (p = 0.97 at 15 weeks, p = 0.97 at 20 weeks, n= 6–9/group). Serial testing of spontaneous alternation (% alternation) did show a significant effect between groups (b, n= 6–9/group). Freezing time (s) in a 24-h fear-conditioning task (c) demonstrated significant differences (p = 0.0003, two-way ANOVA, F = 11.88) with reduced freezing time of both stroke only (*p = 0.013) as well as the 5XFAD transgene (***p = 0.0002). The combined model showed an improvement in memory (**p = 0.008) compared with AD alone. Cumulative cognitive performance measured by combined cognitive z-score (**d**, see “Methods”) demonstrated a similar effect of cognitive enhancement in the combined E4-TR:FAD+ stroke model compared to E4-TR:FAD+ alone (****p < 0.0001)

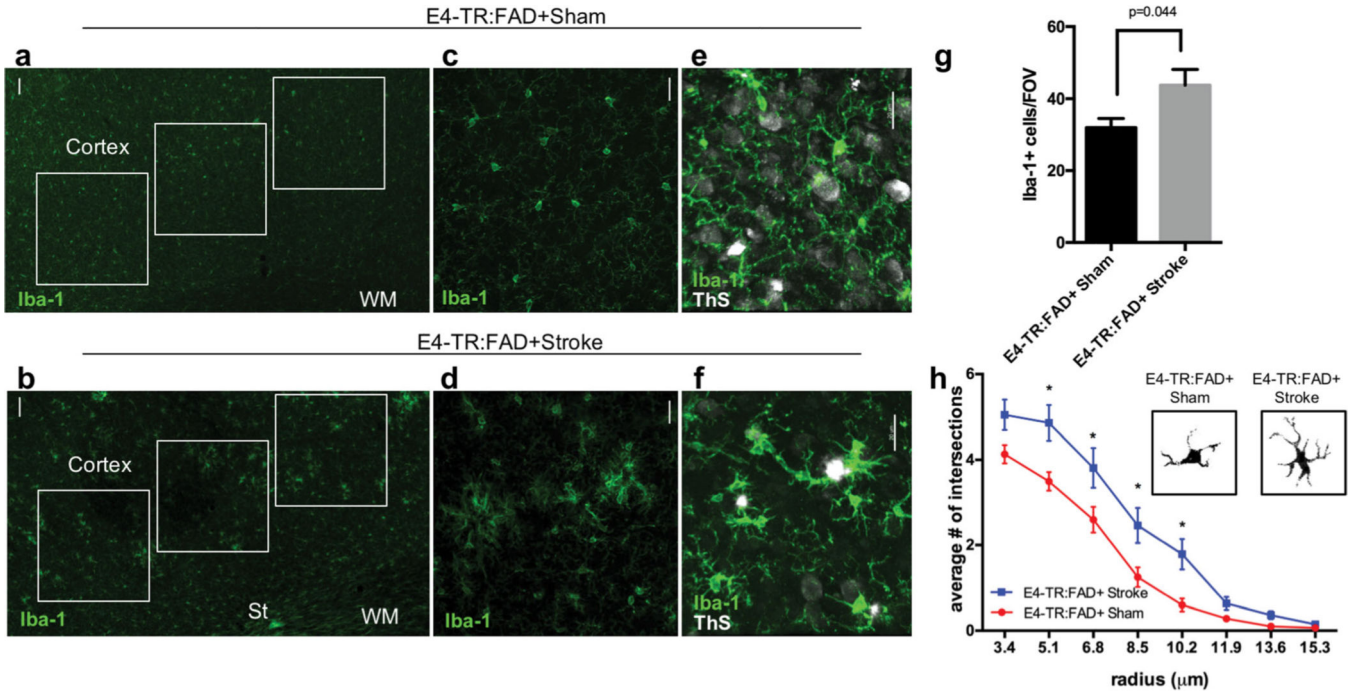

Fig. 5.

Microglial analysis in human ApoE4-TR:5XFAD transgenic mice with subcortical stroke. Immunostaining for Iba-1 in the cortex of 5-month-old E4-TR:FAD+ mice 3 months after the sham (**a, c**) or stroke (**b, d**) procedure. Regions of interest (white boxes) in the ipsilateral cortex were used to quantify the number of Iba1+ cells (**a, b**). Co-labeling with Iba1 (green) and thioflavin S (ThS, white) shows the localization of plaques in relation to Iba1+ cells (**e, f**). Quantification of the number of Iba1-positive cells per field of view (**g**). Microglial morphology measured using Sholl analysis ($n = 45$ cells/animal) demonstrates an increase in activated microglial branching between E4-TR:FAD+ sham and E4-TR:FAD+ stroke ($p < 0.0001$ by two-way ANOVA, $F = 32.09$; *adjusted $p < 0.05$) (**h**). Insets show binary masked examples of microglial morphology from each condition. Scale bars = 50 μm in (**a**) and (**b**); 20 μm in (**c**)–(**f**). St, stroke; WM, white matter; Ve, ventricle

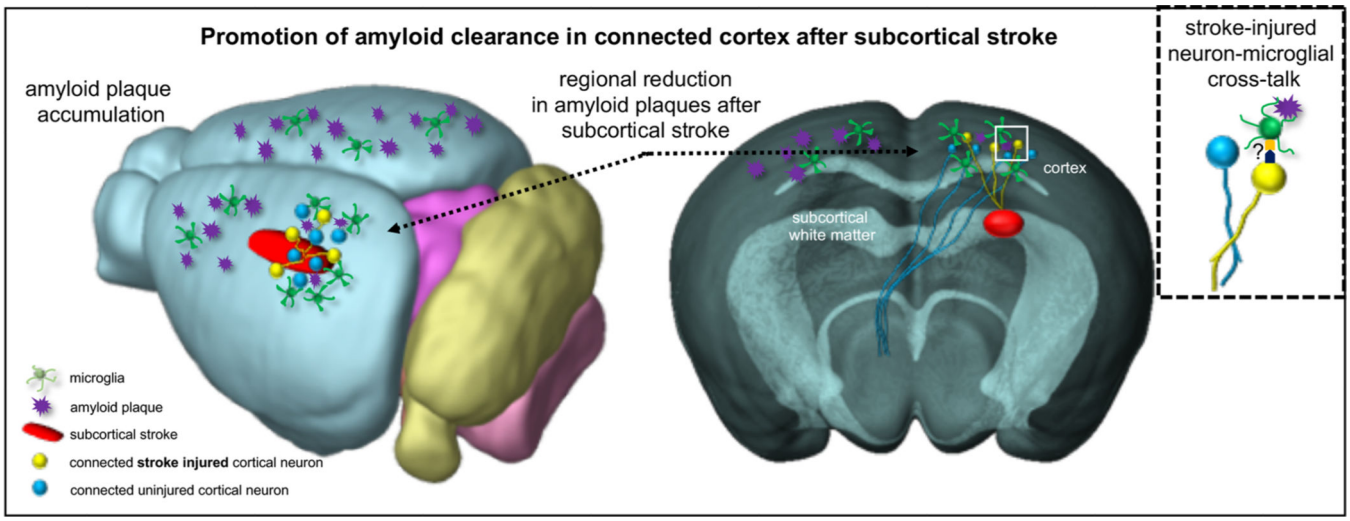

Fig. 6.

Model of the interaction between subcortical white matter stroke and changes in cortical microglial activation and amyloid plaque accumulation. Whole brain (left) and cross-sectional (right) views of the effect of subcortical white matter ischemia on the cortex. The subcortical white matter stroke is shown as a red oblong region. Yellow neurons represent stroke-injured cortical neurons while blue neurons are neighboring un-injured cortical neurons. Amyloid plaques are shown as purple starbursts. Microglial cells are shown in green

Table 1

Study group design by sex, genotype, and assessment with operative mortality

Cohort	Sex	Genotype	Cohort	Mortality (%)
AD (n = 8)	4F/4M	ε4-TR+/+; 5XFAD+	Pathology	0
AD + stroke (n = 9)	3F/6M	ε4-TR+/+; 5XFAD+	Pathology	0
Sham (n = 8)	4F/4M	ε4-TR+/+; 5XFAD−	Behavior	0
Stroke (n = 10)	5F/5M	ε4-TR+/+; 5XFAD−	Behavior	10
AD (n = 13)	7F/6M	ε4-TR+/+; 5XFAD+	Behavior	7.6
AD + stroke (n = 13)	6F/7M	ε4-TR+/+; 5XFAD+	Behavior	7.6